Aggregation, Lipid Exchange, and Metastable Phases of Dimyristoylphosphatidylethanolamine Vesicles†

Celestia Pryor, Mary Bridge, and Leslie M. Loew*

Department of Chemistry, State University of New York at Binghamton, Binghamton, New York 13901

Received April 27, 1984; Revised Manuscript Received August 28, 1984

ABSTRACT: A new fluorescent lipid analogue, bimanephosphatidylcholine, has been synthesized for use in lipid bilayers. This probe is well suited as an energy-transfer donor with *N*-(7-nitro-2,1,3-benzoxadiazol-4-yl)phosphatidylethanolamine as the acceptor. Dimyristoylphosphatidylethanolamine vesicles are prepared by sonication at pH 9 and characterized by electron microscopy and other methods. Resonance energy transfer between separately labeled donor and acceptor vesicles is monitored during HCl-induced aggregation to determine the kinetics of lipid randomization. Light scattering is also monitored to measure the kinetics of aggregation. The light scattering shows a marked reversal with NaOH while the energy transfer does not, indicating lipid exchange during a reversibly aggregated state; the extent of energy transfer suggests that only lipids in the outer monolayers exchange. The gel to liquid-crystalline phase transition temperature in HCl-treated vesicles is found to be 47 °C with diphenylhexatriene. The initial sonicated dispersion does not show a sharp phase transition. In vesicles labeled with both donor and acceptor probes, a small, irreversible increase in energy transfer is obtained upon lowering and then restoring the pH. These results suggest a metastable phase in the sonicated vesicles containing a randomized distribution of lipid and probes within the bilayers; the thermodynamically favored phase, whose formation is triggered by the pH shock, contains domains within which the probe lipids are more highly concentrated.

The diverse behavior of phosphatidylethanolamine (PE)[1] molecules in aqueous dispersions has been the subject of many research efforts which suggest a variety of functional roles for this lipid in cell membranes (Cullis et al., 1982). It has been conjectured, for example, that the nonbilayer phase of PE plays an important role in membrane surface interactions including fusion (Siegel, 1984; Schneider et al., 1980). The phase behavior has been found to be sensitive to temperature, salt concentration, pH, hydrocarbon saturation, and hydrocarbon chain length (Harlos & Eibl, 1981; Mantsch et al., 1981; Seddon et al., 1983; Trauble & Eibl, 1974). PE has been found to form stable bilayers under the proper conditions (Stollery & Vail, 1977). Kolber & Haynes (1979) demonstrated that dimyristoyl- and dipalmitoyl-PE vesicles at pH 9 can be induced to aggregate by dropping the pH to 6. This process was monitored by the decrease in transmitted light and the increase in scattered light which is associated with vesicle aggregation, a necessary precursor to fusion. Fusion is not appreciable as shown by the reversibility of the turbidity upon readjustment to pH 9.

It has also been shown that synthetic DMPE aqueous dispersions adopt a bilayer structure at pH 7 up to 90 °C (Tilcock & Cullis, 1982). Other types of PE which do show a transition to a nonbilayer phase (a hexagonal phase) at pH 7 can be stabilized in the bilayer phase by raising the pH above 8 (Cullis & Dekruijff, 1978; Hardman, 1982). The gel to liquid-crystalline phase transition temperature for DMPE has been reported as various values between 47.5 and 53 °C depending on the method of determination (Wilkinson & Nagle, 1981; Mantsch et al., 1983), but in each case the transition appears sharp.

In this paper, we examine the aggregation process using resonance energy transfer (RET) between labeled vesicle populations. RET is the nonradiative transfer of energy between an electronically excited donor and a ground-state acceptor, the efficiency of which is dependent on the intervening distance. Considerable progress has been made in the study of membrane fusion by employing RET. The quenching of the donor or the enhancement of the acceptor fluorescence is monitored as separately labeled bilayers fuse and the probes are brought close enough to allow RET (Keller et al., 1977; Gibson & Loew, 1979; Deamer & Uster, 1980; Vanderwerf & Ullman, 1980). Alternatively, the loss of RET can be used to watch fusion of colabeled bilayers with blanks (Morgan et al., 1983; Struck et al., 1981). In the present work, the initial findings of which were reported by Pryor et al. (1983), we can monitor lipid exchange within the aggregate. For this experiment, we have developed a new set of RET probes which are relatively insensitive to the pH of the system. The probes are bimanephosphatidylcholine (Bim-PC) and *N*-(7-nitro-2,1,3-benzoxadiazol-4-yl)phosphatidylethanolamine (NBD-PE). These two probes do not readily migrate between bilayers prior to aggregation or fusion.

We also attempt to correlate the aggregation process to changes in the lipid–lipid interactions. This is possible by monitoring the temperature-dependent fluorescence of these head-group probes at the different pHs. This may then be compared to the fluorescence anisotropy of 1,6-diphenylhexatriene (DPH) as a probe of temperature-dependent fluidity

† This work was supported by U.S. Public Health Service Grant CA 23838. L.M.L. is a recipient of Research Career Development Award CA-677 from the National Cancer Institute.

* Address correspondence to this author at the Department of Physiology, University of Connecticut Health Center, Farmington, CT 06032.

[1] Abbreviations: PE, phosphatidylethanolamine; PC, phosphatidylcholine; DM, dimyristoyl; DP, dipalmitoyl; RET, resonance energy transfer; Bim-PC, bimane-PC; NBD-PE, *N*-(7-nitro-2,1,3-benzoxadiazol-4-yl)phosphatidylethanolamine; DPH, 1,6-diphenylhexatriene; T_c, gel to liquid-crystalline phase transition temperature; SUV, small unilamellar vesicle; TLC, thin-layer chromatography; Tris, tris(hydroxymethyl)aminomethane; $diSC_2(5)$, 3,3′-diethylthiodicarbocyanine iodide.

0006-2960/85/0424-2203$01.50/0

within the hydrocarbon region (Lentz et al., 1976; Lentz & Litman, 1978).

Materials and Methods

Synthesis of Bim-PC. Bim-PC was synthesized by reacting 28 mg of monobromobimane (Kosower et al., 1978) (Calbiochem Behring, San Diego, CA) with 70 mg of dipalmitoyl-L-α-phosphatidyl-*N*,*N*-dimethylethanolamine (Calbiochem Behring) in 3 mL of CH_3CN (dried over 4-Å molecular sieves) and 1 mL of $CHCl_3$ (purified by passage through a column of neutral alumina) to which was added 30 μL of diisopropylethylamine (Aldrich Chemical Co., Milwaukee, WI). The reaction mixture was refluxed for ~115 h. During this time, the mixture was checked by TLC (chloroform/methanol/water, 65:25:4, R_f 0.89) to determine the progress of the reaction. The reaction was terminated when a single fluorescent spot remained. Two preparative TLC's on 2000-μm silica gel plates, first with the solvent mixture acetone/water (85:5) and then with chloroform/methanol/ammonium hydroxide (65:25:4), are required for purification. The yellow product band was scraped off the plate and the product extracted by stirring with 50 mL of chloroform/methanol (2:1) and 1–2 drops of HCl. This was then filtered to remove any suspended silica gel and the solvent evaporated under reduced pressure providing 24 mg of product. The product was then dried and stored in the freezer as an ethanol solution. A phosphate analysis provided the final concentration [Fiske & Subbarow, 1925; modified by Bartlett (1958) and Litman (1973)].

DMPE Vesicle Preparation. Synthetic DMPE and NBD-PE were purchased from Avanti Biochemicals, Birmingham, AL. Chloroform solutions containing 2 μmol of lipid plus the appropriate fluorescent probe were dried under a stream of nitrogen and then placed in a vacuum desiccator for 3 h to remove final traces of solvent. The mixture was resuspended in 10 mL of 10 mM Tris buffer at pH 9. The sample was sonicated with a Branson W185 probe sonifier under N_2 or Ar for 15 min at 60 °C; the resulting dispersions are generally clear. The separately labeled vesicles contained 1 mol % NBD-PE and 2 mol % Bim-PE, respectively, while the colabeled vesicles contained only 0.5 mol % NBD-PE and 1 mol % Bim-PE to achieve the same final level of fluorescence.

Fluorescence Experiments. Stopped-flow fluorescence, light scattering, and transmittance were measured simultaneously with two photomultiplier tubes and a photodiode positioned on an Aminco stopped-flow device (from SLM-AMINCO, Urbana, IL). The fluorescence and light-scattering pathways were each 5 mm long at 90° to the incident light, and the transmittance path was 2 mm long in line with the incident path. A monochromator at 380 nm was used to select the exciting wavelength, and a 550-nm cutoff filter was used to select the NBD fluorescence emission. Other fluorescence and light-scattering work was done with a Perkin-Elmer MPF-44B fluorescence spectrometer and a Bascom-Turner digital recorder. The excitation monochromator was set at 380 nm to excite the bimane chromophore, and the fluorescence emission was either scanned from 425 to 600 nm or set at a single wavelength. Emission spectra were corrected. Vesicle aggregation was monitored by the light scattering at 380 nm. The vesicles prepared at pH 9 were induced to aggregate by addition of HCl to approximately pH 6. The reversibility was tested by readjustment to pH 9 with NaOH.

Lipid Phase Studies. The temperature dependence of light scattering and the fluorescence of the head-group probes were determined at each stage of the pH cycle (pH 9 → pH 6 → pH 9) in the PE dispersions. A thermistor probe (YSI Model 425C from Telethermometer, Yellow Springs Instrument Co., Inc.) was placed directly in the cuvette and provided the *x* axis. The fluorescence or light scattering provided the *y* axis. In addition, the fluorescence anisotropy of DPH vs. temperature was determined on a point by point basis to observe the gel to liquid-crystalline phase transition. A 1.5-μL aliquot of 4 mM DPH (Molecular Probes, Junction City, OR) in tetrahydrofuran was added to a 3-mL sample of the vesicle preparation for these experiments; Polacoat film polarizers supplied by Perkin-Elmer were employed with excitation at 360 nm and emission at 430 nm.

Characterization of Vesicles. PE vesicles were made at high concentration in 50 mM K_2SO_4 buffer (10 mM Tris, pH 9) and diluted into 50 mM Na_2SO_4 buffer (10 mM Tris, pH 9). Valinomycin (Calbiochem) was added to induce K^+ permeability. This creates a membrane potential which is detectable with the fluorescent probe $diSC_2(5)$ (Sims et al., 1974). The potential can be eliminated by the addition of gramicidin (Sigma) which allows Na^+ transport, restoring the original value (control experiments with external K^+ buffer show no fluorescence changes upon addition of either ionophore). This technique indicates the presence of closed bilayer structures. Electron micrographs were taken of the vesicle preparation with a Philips 101 microscope. The samples were negatively stained with 3% ammonium molybdate.

A Fiske–Subbarow phosphate analysis (Fiske & Subbarow, 1925) was used with modification by Bartlett (1958) and Litman (1973) to determine all final lipid concentrations.

Results

DMPE Vesicle Characterization. There have been some reports in the literature of unsuccessful attempts to prepare vesicles from pure PE (Litman et al., 1973). However, Stollery & Vail (1977) and Kolber & Haynes (1979) have reported vesicle formation. The hexagonal phase appears to dominate with long-chain and/or unsaturated PE molecules. This work deals only with synthetic DMPE which contains short (14 carbon) saturated fatty acids.

In an effort to characterize our lipid dispersion, we obtained electron micrographs of negatively stained samples (Figure 1). These micrographs reveal vesicle structures at both low and high pH. Under the acid conditions (pH 6), large aggregates are present, as expected, which are apparently dispersed upon readjustment to high pH (panels b and c, respectively, of Figure 1). The long thin structures in Figure 1c are remarkably similar to those found by Parente & Lentz (1984) for PC vesicles and may be vesicles which have collapsed before staining. In addition, analyses of micrographs taken before and after a complete pH cycle indicate no significant change in average vesicle size. An average diameter of 510 Å was obtained for the initial vesicle preparation with a standard deviation of 242 Å (59 vesicles measured). A micrograph containing 42 vesicles from a sample that had been through a complete pH cycle gave an average diameter of 520 ± 150 Å. Analysis of the size distribution in a set of three micrographs obtained before and after the pH cycle appears to indicate a more uniform vesicle population after the cycle; a much larger sample is necessary to be sure of the significance of this observation, however. As further evidence for vesicle formation, the generation of a membrane potential can be demonstrated as described under Materials and Methods. Clearly, this ability of the lipid dispersion to maintain a diffusion potential would not be possible without at least some closed membrane structures. The cation gradients are not preserved through a pH cycle; this is consistent with the finding of Ellens et al. (1984) in a study of leakage upon acid-mediated

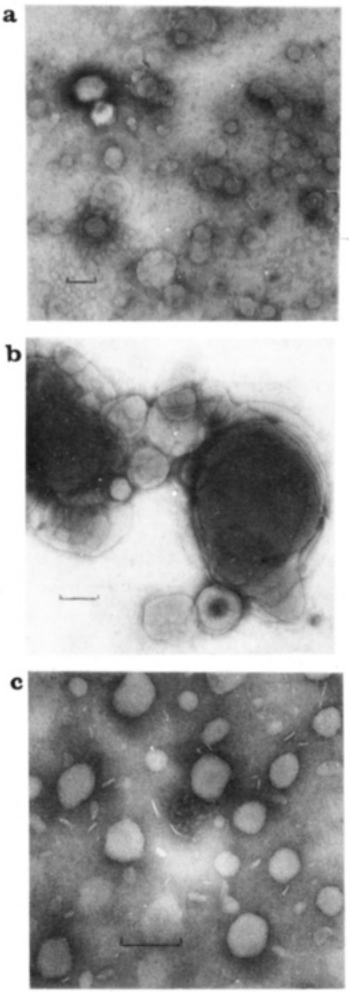

FIGURE 1: Transmission electron micrograph of sonicated PE dispersions negatively stained with 3% ammonium molybdate. The bar in each micrograph represents 1000 Å. (a) Initial dispersion at pH 9; (b) after dropping to pH 6 with HCl; (c) after returning to pH 9 with NaOH.

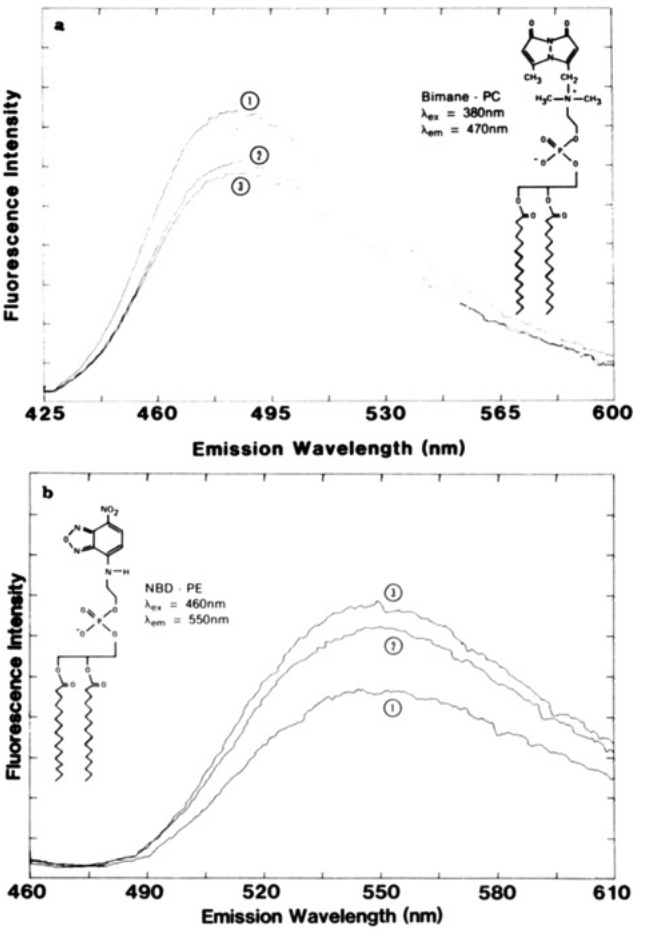

FIGURE 2: Corrected emission spectra of labeled DMPE vesicles. (a) A 50:50 mixture of Bim-PC and unlabeled DMPE vesicles is excited at 380 nm and scanned from 425 to 600 nm. The inset shows the structure of Bim-PC. (b) A 50:50 mixture of NBD-PE and unlabeled DMPE vesicles is excited at 440 nm, and the emission is scanned from 460 to 610 nm. The inset shows the structure of NBD-PE. Curve 1, initial vesicle preparation, pH 9; curve 2, after addition of HCl, pH 6; curve 3, after addition of NaOH, pH 9. Dilutions resulting from acid and base additions are insignificant.

aggregation of PE vesicles containing cholesteryl hemisuccinate.

Two encapsulation experiments were attempted but were unsuccessful. Carboxyfluorescein (Ralston et al., 1981) appears to leak from the vesicle on passage of the sample through a Sephadex column. This seems to result from disruption of the vesicles on the column since the lipid is strongly retained, trailing over many fractions past the void volume. A procedure for quenching of external calcein with Co^{2+} (Oku et al., 1983) is accompanied by massive light-scattering changes presumably due to aggregation or fusion of the vesicles. Despite these results, the micrographs and the diffusion potential experiments provide convincing evidence that vesicles can be prepared at pH 9.

NBD-PE and Bim-PC as RET Probes. We have found NBD-PE and Bim-PC to be useful as RET probes in vesicle systems. They are relatively insensitive to pH, having no groups with p*K*s in the range of pH 6–9. Their large Stokes shifts are convenient to efficiently monitor energy transfer—an advantage over the NBD-rhodamine system (Struck et al., 1981). They are small chromophores (compared to fluorescein or rhodamine, for example) and threfore may cause only slight perturbations to the head-group region of the bilayers and even less to the interior. Both probes are tightly bound to the bilayer and do not readily diffuse from one vesicle to another across the bulk solution; there is no change in energy transfer upon incubating equal volumes of separately labeled vesicles over periods of 30 min or more.

Figure 2 shows the probe structures along with their emission spectra when bound to the PE vesicles. It is evident that the probes' fluorescence does change somewhat with pH but this reflects changes in the lipid environment (discussed in detail later) rather than any significant intrinsic pH sensitivity of either chromophore. Note, specifically, that the change observed upon decreasing the pH does not reverse when the original pH is restored.

The critical transfer distance, R_0, for this probe pair has been calculated by using two independent methods. The theoretical relationship of R_0 to the overlap of the donor emission and acceptor absorption spectra, as described by Förster (1959), gives an R_0 of 24.3 Å (orientation assumed random). Donor fluorescence quenching was determined experimentally in lipid vesicles colabeled with the probes. Analysis of these data by the two-dimensional approximate treatment of Estep & Thompson (1979), which assumes a random distribution, provided a value of 25 Å for R_0. The agreement between these two determinations of R_0 suggests that the probes are randomly distributed in the PE pH 9 vesicles.

RET between Bim-PC and NBD-PE Vesicles Induced by a pH Drop. Separately labeled vesicles at pH 9 were excited at 380 nm, and the fluorescence emission was scanned from

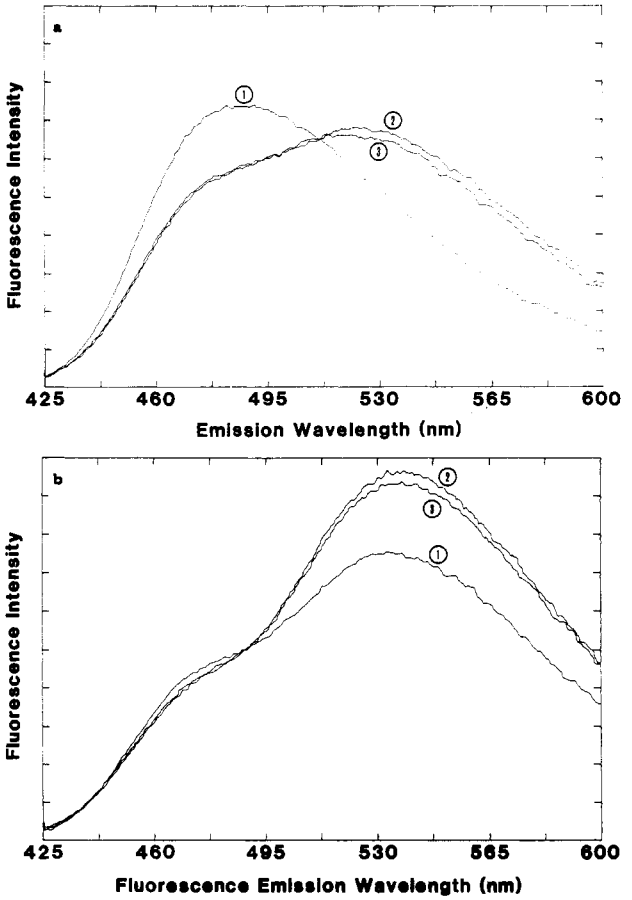

FIGURE 3: Fluorescence energy transfer induced by pH drop. Excitation at 380 nm. (a) 1:1 mixture of separately labeled Bim-PC and NBD-PE vesicles; (b) colabeled Bim-PC/NBD-PE vesicles. Curve 1, initial vesicle preparation, pH 9; curve 2, after addition of HCl, ~pH 6; curve 3, after addition of NaOH, ~pH 9. Dilution differences as a result of the acid and base additions are insignificant.

425 to 600 nm (Figure 3a, curve 1). HCl was added to drop the pH to 6 and the fluorescence scanned again. At this point, the Bim-PC fluorescence is quenched while the NBD-PE fluorescence is enhanced (Figure 3a, curve 2). This effect is due to energy transfer at the lower pH and indicates that the probes have been brought into close proximity. The addition of NaOH to reverse the pH to 9 (Figure 3a, curve 3) shows that the fluorescence does not return to the original levels. Figure 3b follows the same sequence with colabeled vesicles. Here, energy transfer is clearly in evidence before aggregation (Figure 3b, curve 1). The addition of HCl causes a small increase, possibly due to the increased density of fluorescent probes in the aggregate or the development of domains in which the probes are concentrated (Figure 3b, curve 2). This also is not appreciably reversible with NaOH (Figure 3b, curve 3). Note that RET in the separately labeled vesicles is never as large as in the colabeled vesicles, while both samples contain the same amount of fluorescent material and lipid. Analysis of the data in Figure 3 shows that, on the basis of the bimane emission at 470 nm, the energy transfer in the separately labeled vesicles amounts to only 57% of the maximum level attained in the colabeled vesicles at pH 6. A similar analysis for the enhancement of NBD fluorescence at 550 nm in the separately labeled vesicles shows only 46% of the maximum. A control experiment, not shown, involves the addition of premixed HCl and NaOH (same amounts as used in the previous experiments); no change in either fluorescence or light scattering is seen, indicating that neither interactions with the added ions nor osmolarity variations contribute to the results.

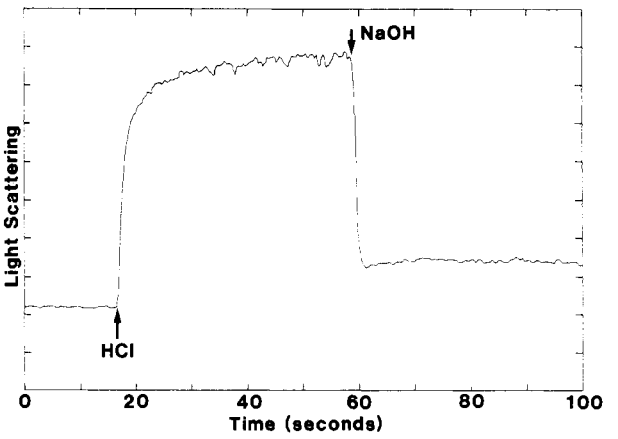

FIGURE 4: Light scattering of unlabeled vesicles monitored at 380 nm. The HCl and NaOH additions cause less than 1% dilution. Note the recovery is greater than 80%.

That the aggregation process itself is largely reversible can be seen by following light scattering (Figure 4). Scattered light is collected at 90° from the 380-nm beam incident on unlabeled vesicles. As the pH is dropped, the light scattering increases to a large extent, showing that the relative particle size becomes much larger. Addition of NaOH induces nearly complete (80–85%) reversal, showing that these aggregates can be dissociated. These results are consistent with those of Kolber & Haynes (1979).

Stopped-flow experiments were performed to define the time course of these processes. Three channels display changes in transmission, scattering, and fluorescence. Figure 5a shows the results of mixing separately labeled vesicles with HCl. The fluorescence increase can best be fitted to a hyperbolic function consistent with a rate-limiting bimolecular reaction. Figure 5b shows the nonlinear least-squares fit obtained to an equation of the form

$$F(t) = \frac{a/c}{1 + 1/kat} - F(0) \qquad (1)$$

where $F(t)$ is the fluorescence of NBD at time t, k is the second-order rate constant, a is the initial concentration of vesicles, and c is the proportionality constant relating the extent of dimerization to the enhancement of NBD fluorescence. The fit to eq 1 is significantly better than that obtained by an attempt to fit the data to a single exponential ($p < 0.05$; F test). The rate-determining step thus appears to be the dimerization of the vesicles. An actual rate constant for the dimerization requires an estimate of the vesicle concentration; the size analysis of the vesicles in the electron micrographs and a phosphate analysis to determine lipid concentration can be combined with the value of 42 Å^2 occupied by a PE molecule in a bilayer (Jain & Wagner, 1980) to provide this information. The stopped-flow experiments lead to a rate constant at 25 °C (averaged over six separate experiments) of $(1.1 \pm 0.3) \times 10^9$ M^{-1} s^{-1}. If the fit is attempted with the light-scattering data, contamination from higher order aggregation complicates the analysis, but similar rates are obtained. These results clearly indicate that vesicle dimerization is slow compared to the subsequent probe intermixing. This rate constant is faster than that reported by Kolber & Haynes (1979) from their light-scattering results (2×10^7 M^{-1} s^{-1}). The discrepancy may be due to the different approaches taken to estimate the vesicle concentration or the possibility that the size of the pH jumps was not the same in these poorly buffered systems. In a separate experiment (not shown), colabeled vesicles are mixed with HCl. The kinetic traces obtained have

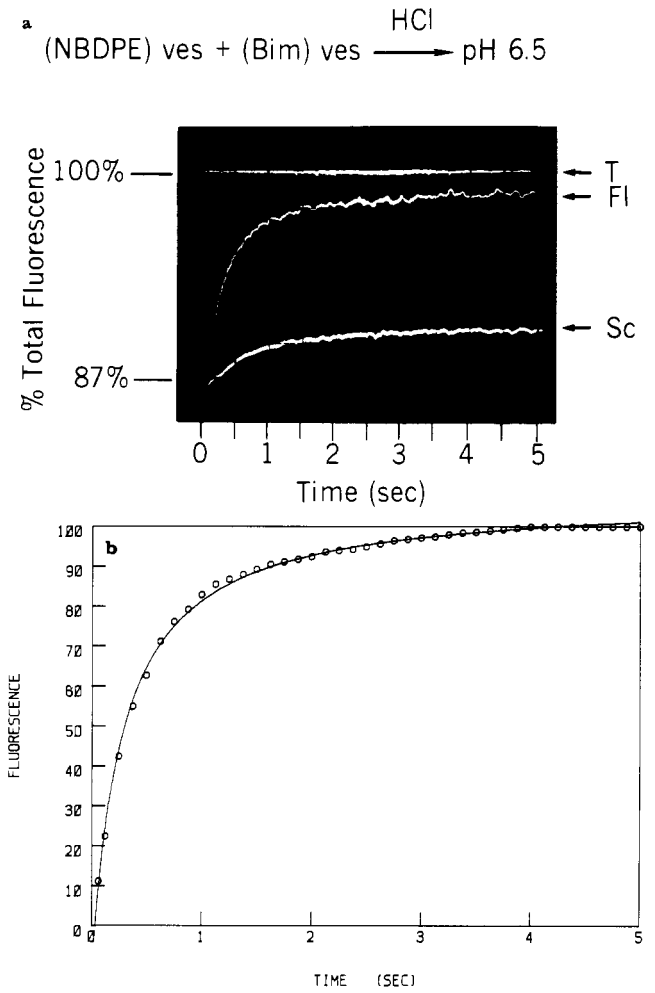

FIGURE 5: (a) Stopped-flow kinetics of the transmission, fluorescence, and light scattering of a separately labeled mixture of NBD-PE and Bim-PC DMPE vesicles rapidly mixed with HCl. The sample is excited at 380 nm, and the fluorescence is selected with a 550-nm cutoff filter. The scale refers to the fluorscence change (Fl) with 100% set at the infinity point. Scattering and transmittance channels are indicated by Sc and T, respectively. (b) Fit of the fluorescence change to a second-order rate equation. Data points are indicated by (O).

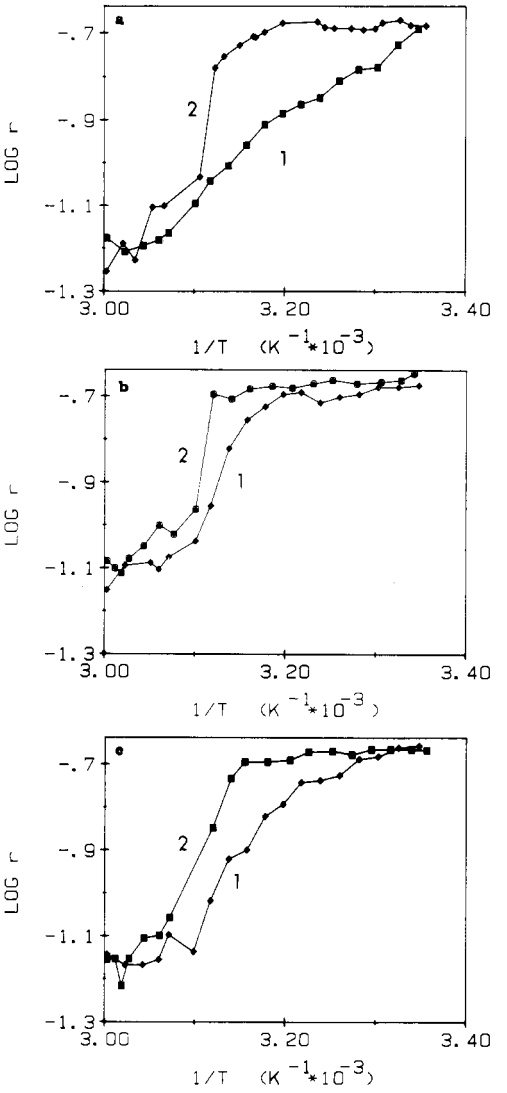

FIGURE 6: Fluorescence anisotropy, r, of 2 mol % DPH in the DMPE vesicle preparation as a function of temperature. The data are presented as a pseudo-Arrhenius plot to accentuate the phase transitions. (a) DMPE vesicles, pH 9; (b) after addition of HCl, pH 6; (c) after addition of NaOH, pH 9. Curve 1, cooling from 60 to 25 °C; curve 2, heating from 25 to 60 °C.

smaller amplitudes (as expected from the results in Figure 3) and fit a single exponential ($\tau = 63 \pm 4$ ms) better than the hyperbolic function ($p < 0.05$). This indicates different mechanisms cause the acid-mediated increase of RET in the two systems; presumably, the process occurring in the colabeled systems is also occurring in the separately labeled vesicle experiments but is simply masked by the larger change in RET which we have attributed to probe mixing.

Lipid Phase Behavior. To further define this lipid system, the temperature-dependent fluorescence anisotropy of DPH was investigated to detect any phase transitions. Diphenylhexatriene (DPH) has been previously used as a fluidity probe in mixed PE/PC vesicles (Lentz et al., 1976). The rod-shaped molecule inserts into the hydrocarbon portion of the membrane, and the fluorescence anisotropy is dependent on the motional freedom of the molecule. The transition from the liquid-crystalline phase to the gel phase imparts a tighter ordering to the hydrocarbon chains. This limits the motional freedom of the DPH, and hence, the fluorescence anisotropy displays an abrupt discontinuity at the temperature of the phase transition. PE vesicles prepared in pH 9 buffer at 55 °C and maintained at that temperature until commencement of the anisotropy measurements displayed no distinct phase transition upon cooling but did show a transition at 48 °C upon subsequent reheating (Figure 6a). Vesicles treated with HCl (Figure 6b) and vesicles subjected to the entire pH cycle (Figure 6c) displayed distinct transitions in both their heating and their cooling curves; the transition temperature is surprisingly insensitive to pH.

The light scattering and probe fluorescence were also measured as a function of temperature. Vesicles at pH 9 show a slight increase in light scattering as the temperature is cooled from 60 to 25 °C. The heating scan is nearly superimposable. Upon addition of HCl to pH 6, the change in light scattering is greatly increased in both the heating and cooling scans. This behavior is not reversed by addition of NaOH to pH 9. The T_c's found by this means were all slightly lower than with DPH (47 °C). This method monitors overall changes in the vesicle size or shape.

The head-group probes' fluorescence may be sensing organizational changes in their immediate environment. Results from bimane-labeled vesicles are shown in Figure 7 and are quite similar to experiments with either direct or sensitized NBD fluorescence as a probe. The heating and cooling scans are very different, and there is a pronounced effect of lowering the pH to 6. Raising the pH back to 9 does not promote

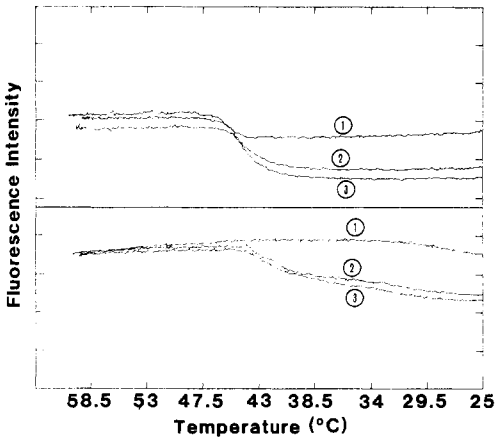

FIGURE 7: Temperature-dependent behavior of Bim-PC fluorescence in DMPE vesicles excited at 380 nm and monitored at 460 nm. (Bottom) Cooling curves, 60–25 °C; (top) heating curves, 25–60 °C. Curve 1, 50:50 mixture of Bim-PC and unlabeled DMPE vesicles, pH 9; curve 2, after addition of HCl, pH 6; curve 3, after addition of NaOH, pH 9.

recovery of the original temperature-dependent behavior. As for the DPH anisotropy experiments, the traces corresponding to cooling of the initial high-pH vesicles do not contain discontinuities in the temperature range of the phase transition.

Thus, the temperature dependence of several parameters, which report on different aspects of the state of the PE dispersion, has been monitored. Whether sensitive to motional freedom in the hydrocarbon region, the microenvironment in the head-group region, or the overall size and shape of the particles in the lipid dispersion, all these parameters display a consistent pattern: the original high-pH dispersion does not have a distinct transition in the cooling curve but does indicate a sharp phase change upon reheating; lowering the pH produces sharp transitions in both halves of the temperature cycle which are preserved when the original pH is restored. The temperature of the transition is in the range of that reported for the gel to liquid-crystal transition determined in careful calorimetric studies (Wilkinson & Nagle, 1981; Mantsch et al., 1983).

DISCUSSION

Vesicle–vesicle surface interactions during aggregation have been monitored by the resonance energy transfer between surface probes. The stopped-flow kinetics (Figure 5) fit a second-order rate equation corresponding to the dimerization of the vesicles. The light-scattering change, which depends directly on particle size, follows a similar time course, indicating that vesicle aggregation is the rate-limiting process. Once the membranes are in contact, a fast exchange of the fluorescent lipids occurs allowing a large increase in RET. The rate found by fitting the data to a second-order integrated rate equation is $(1.1 \pm 0.3) \times 10^9$ M^{-1} s^{-1} at 25 °C. This may be compared to the diffusion-controlled rate of 2.9×10^9 M^{-1} s^{-1} calculated for vesicle dimerization under these conditions.

The level of RET seen in the separately labeled aggregated system is always lower than that of the colabeled system, while both sets show little reversibility (Figure 3). Thus, the separately labeled vesicles never reach the completely random distribution of probe molecules found in the colabeled system even at times sufficient for extensive development of higher order aggregation or when the pH cycle is repeated.

It is possible that this result arises from fusion of some but not all of the vesicles in the preparation; perhaps the smaller vesicles have a tendency to fuse subsequent to aggregation while initially large vesicles do not. Although this possibility

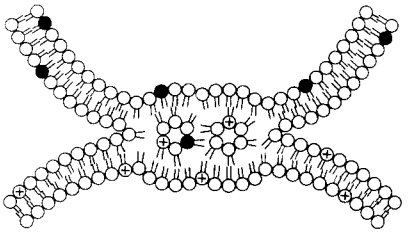

FIGURE 8: Proposed model for fluorescent lipid analogue exchange between vesicle outer monolayers.

is weakened by the near invariance in the vesicle size distribution from the electron micrographs (Figure 1) and the high degree of reversibility in the light scattering (Figure 4), it cannot be ruled out; there is, after all, a small increase in mean vesicle diameter accompanying an apparent decrease in size heterogeneity. Further, the irreversibility of the pH-dependent phase behavior (Figures 6 and 7) may be interpreted in terms of a depletion of the population of small vesicles. We have, however, taken the separately labeled vesicles through the pH cycle before mixing. If limited fusion of small vesicles is the origin of the RET (seen in Figure 3a), these preconditioned vesicles should not develop significant RET after mixing and pH cycling: the RET develops to an extent equivalent to that of fresh vesicles. Thus, limited fusion cannot be the sole origin of the limited extent of the RET which accompanies aggregation of separately labeled vesicles.

Another possibility is that the interaction of the membranes, and indeed the lipid exchange, is confined to the outer monolayer. The aggregation is a necessary precursor to the exchange as no energy transfer develops upon prolonged incubation of the vesicles at pH 9. Figure 8 shows a model of vesicle interaction where the outer monolayers form a hexagonal or reverse micelle region. This has been proposed as a step in the mechanism of fusion by Cullis et al. (1981) and by Siegel (1984). This model allows only 60% of the maximum RET to be attainable upon aggregation of separately labeled vesicles since the probes in the inner monolayers cannot exchange and thus cannot reach proximity to their respective RET partners. The value of 60% corresponds to the surface area of the outer relative to the inner monolayer based on the average vesicle dimensions determined from the electron micrographs. Experimentally, energy transfer in the separately labeled vesicles never exceeds 57% of that attained in the colabeled vesicles containing the same concentration of donor and acceptor probes.

This model of vesicle–vesicle interaction can describe the kinetics and final levels of RET seen in these experiments. However, we have yet to account for all of the irreversible behavior seen during the pH cycle. This irreversibility is present in the RET, the DPH anisotropy, the pH-dependent changes in the head-group probe spectra, and the temperature dependence of probe fluorescence, as seen in Figures 3b, 6, 2, and 7, respectively. The colabeled vesicles display a small but significant increase in RET upon addition of HCl which does not reverse completely at the end of the pH cycle, indicating that the distance between the probes has been altered by the cycle. The very fact that the colabeled vesicles undergo any increase in RET shows that lipid exchange via aggregation is not the only process occurring in the preparation. Further support for the assertion that the RET in Figure 3b is reporting on the states of the lipids, as opposed to changes in the fluorescent probes, is that DPH anisotropy measurements show an irreversible pH effect on the lipid phase transition. Figure 6a shows no distinct transition for the cooling of vesicles at pH 9. The heating and cooling cycle is reproducible at this

stage. The pH drop to 6 changes the DPH anisotropy so that the cooling curve now displays a distinct transition (Figure 6b). The reverse to pH 9 does not remove this transition (Figure 6c).

The addition of HCl causes a change in the lipid–probe and/or lipid–lipid relationships, leading to a more stable state. We believe that this is an alteration in the lipid–lipid interactions leading to exclusion of the fluorescent lipid analogues into lateral domains in the vesicle bilayers. Also consistent with these data is the pH/temperature-dependent behavior of the fluorescent head groups. Figure 7 shows the change in Bim-PC fluorescence due to temperature and pH. Cooling scan 1 (the initial vesicle preparation) has no distinct transition while scans 2 (after HCl) and 3 (after reversal) both display inflections close to the expected temperature. The pattern is similar to that of the DPH experiments. NBD-PE fluorescence shows a similar pattern of irreversible phase behavior induced by the pH drop. A temperature dependence of light scattering at 90° also displays this same pattern: The initial sample does not display much change in light scattering from 60 to 25 °C. However, upon addition of HCl, a dramatic change in light scattering is seen as the bilayers pass through the liquid-crystalline to gel transition. This transition is not abolished by addition of NaOH.

These light-scattering results are obtained in the absence of any probe. The consistent pattern of behavior observed via all of these techniques appears likely, therefore, to reflect intrinsic changes in the state of the DMPE rather than artifactural effects resulting from probe perturbations. It is possible to conclude that the irreversible increase in probe proximity, indicated by the results in Figure 3b for the colabeled vesicles, and the permanent alterations in the lipid phase behavior reported by DPH (Figure 6) may have the same origin. The polymorphism available to DMPE and the possibility of a metastable state at these temperatures have been recently described by Wilkinson & Nagle (1984) in a calorimetric investigation of hydrated DMPE multilayers.

Thus, a complex model for the behavior of DMPE vesicles emerges. The high-pH sonicated vesicles are initially in a metastable state in which any lipid probes are randomly distributed. The HCl induces formation of domains of the fluorescent lipids as well as the aggregation of the vesicles. The RET kinetics of the separately labeled system are dominated by probe mixing with dimerization as the rate-controlling step while the colabeled RET kinetics are controlled by the formation of domains subsequent to H^+-catalyzed relaxation from the initial metastable states. The phase behavior of the lipid reflects this same relaxation. Clearly, other models can be devised which can rationalize all of the data. The model proposed here, however, has the advantage of a strong foundation in earlier experimental and theoretical investigations of the phosphatidylethanolamine–water system.

ACKNOWLEDGMENTS

Valuable comments on an earlier version of the manuscript were obtained from D. Haynes, J. Silvius, F. Szoka, D. Wilkinson, and the referees.

REFERENCES

Bartlett, G. R. (1948) *J. Biol. Chem. 234*, 466–468.

Cullis, P. R., & deKruijff, B. (1978) *Biochim. Biophys. Acta 513*, 31–42.

Cullis, P. R., Farren, S. B., & Hope, M. J. (1981) *Can. J. Spectrosc. 26*, 89–95.

Cullis, P. R., deKruijff, B., Hope, M. J., Verkleij, A. J., Nayar, R., Farren, S. B., Tilock, C., Madden, T. D., & Bally, M. P. (1982) in *Membrane Fluidity in Biology: Concepts of Membrane Structure* (Aloia, R. C., Ed.) Vol. 2, Academic Press, New York.

Deamer, D. W., & Uster, P. S. (1980) in *Introduction of Macromolecules into Viable Mammalian Cells*, pp 205–220, Alan R. Liss, New York.

Ellens, H., Bentz, J., & Szoka, F. C. (1984) *Biochemistry 23*, 1532–1538.

Estep, T. N., & Thompson, T. E. (1979) *Biophys. J. 26*, 195–208.

Fiske, C. H., & Subbarow, Y. (1925) *J. Biol. Chem. 66*, 375–400.

Förster, T. (1959) *Discuss. Faraday Soc. 27*, 7–17.

Gibson, G., & Loew, L. (1979) *Biochem. Biophys. Res. Commun. 88*, 135–140.

Hardman, P. D. (1982) *Eur. J. Biochem. 124*, 95–101.

Harlos, K., & Eibl, H. (1981) *Biochemistry 20*, 2888–2892.

Jacobson, K., & Papahadjopoulos, D. (1975) *Biochemistry 14*, 152–161.

Jain, M. K., & Wagner, R. C. (1980) *Introduction to Biological Membranes*, Wiley, New York.

Kolber, M. A., & Haynes, D. H. (1979) *J. Membr. Biol. 48*, 95–114.

Kosower, E. M., Pazhenchevsky, B., & Kershkowitz, E. (1978) *J. Am. Chem. Soc. 100*, 6516–6518.

Lentz, B. R., & Litman, B. J. (1978) *Biochemistry 17*, 5537.

Lentz, B. R., Barenholz, Y., & Thompson, T. E. (1976) *Biochemistry 15*, 4521–4529.

Litman, B. J. (1973) *Biochemistry 12*, 2545–2554.

Mantsch, H. H., Martin, A., & Camerson, D. G. (1981) *Biochemistry 20*, 3138–3145.

Mantsch, H. H., Hsi, S. C., Butler, K. W., & Camerson, D. G. (1983) *Biochim. Biophys. Acta 728*, 325–330.

Morgan, C. C., Thomas, E. N., & Yianni, Y. P. (1983) *Biochim. Biophys. Acta 728*, 356–362.

Oku, N., Kendall, D. A., & MacDonald, R. C. (1982) *Biochim. Biophys. Acta 691*, 332–340.

Parente, R. A., & Lentz, B. R. (1984) *Biochemistry 23*, 2353–2362.

Pryor, C. L., Loew, L. M., & Bridge, M. (1983) *Biophys. J. 41*, 349a.

Ralston, E., Hjelmeland, L. M., Lkausner, R. D., Weinstein, J. N., & Blumenthal, R. (1981) *Biochim. Biophys. Acta 649*, 133–137.

Schenider, H., Lemasters, J. J., Hochli, M., & Hackenbrock, C. R. (1980) *Proc. Natl. Acad. Sci. U.S.A. 77*, 429–496.

Seddon, J. M., Ceyc, G., & Marsh, D. (1983) *Biochemistry 22*, 1280–1289.

Siegel, D. P. (1984) *Biophys. J. 45*, 399–420.

Sims, P. J., Waggoner, A. S., Wang, C., & Hoffman, J. F. (1974) *Biochemistry 13*, 3315–3330.

Stollery, J. G., & Vail, W. J. (1977) *Biochim. Biophys. Acta 471*, 372–390.

Struck, D. K., Hoekstra, D., & Pagano, R. E. (1981) *Biochemistry 20*, 4093–4099.

Tilcock, C. P. S., & Cullis, P. R. (1982) *Biochim. Biophys. Acta 684*, 212–218.

Trauble, H., & Eibl, H. (1974) *Proc. Natl. Acad. Sci. U.S.A. 71*, 214–219.

Vanderwerf, P., & Ullman, E. F. (1980) *Biochim. Biophys. Acta 596*, 302–314.

Wilkinson, D. A., & Nagle, J. F. (1981) *Biochemistry 20*, 187–192.

Wilkinson, D. A., & Nagle, J. F. (1984) *Biochemistry 23*, 1538–1541.